Electrochimica Acta 439 (2023) 141674

Contents lists available at ScienceDirect

Electrochimica Acta

journal homepage: www.journals.elsevier.com/electrochimica-acta

Template-free electrochemical deposition of tellurium nanowires with eutectic solvents

Samuel C. Perry *, Joshua White, Iris Nandhakumar

Department of Chemistry, University of Southampton, Southampton, SO17 1BJ. UK

ARTICLE INFO

Keywords:
Deep eutectic solvents
electrodeposition
tellurium
nanowires
nanoplatelets

ABSTRACT

Electrochemical deposition of tellurium from deep eutectic solvents (DES) at gold film electrodes produced films of tellurium nanowires. The deposition was evenly distributed over the gold surface, with an average diameter of ~70 nm and length of ~1 μm. Deposition was extremely sensitive to the applied potential, tellurium concentration and deposition bath temperature, with deviations away from optimised conditions preventing the formation of the desired nanostructure. Interestingly, replacing the chloride in a popular eutectic solvent with bromide or iodide had a significant impact on the resultant film structure, with bromide giving no clearly defined nanostructure but iodide giving nanoplatelets. This demonstrates a strong control of tellurium nanostructure by halide ions, offering a way to two distinct nanostructures from the same core experimental set up.

1. Introduction

Tellurium (Te) nanostructures are attracting increasing interest across thermoelectric, piezoelectric and optoelectronic fields [1,2]. In all cases, producing low dimensional nanostructures such as nanorods or nanowires enables the development of materials that far exceed the performance of the analogous bulk materials [3,4]. This had led to increased interest in developing ways of efficiently producing arrays of low dimensional Te nanostructures.

One of the more commonly employed synthesis routes is solvothermal synthesis, where strong reductants in an inert atmosphere reduce Te precursors in the presence of dissolved templating agents such as polyvinylpyrrolidone in order to guide the production of wires [5]. This is an effective method to produce large yields of low order nanostructures, but also requires costly high temperature and low pressure equipment in order to function.

Alternatively, it is possible to produce nanowires by electrodepositing materials through a porous template made of aluminium oxide, polycarbonate or another similar material that can be later removed through a dissolution process [6]. These produce very ordered arrays of similar wires, although challenges surrounding pore filling can hinder growth, particularly when using templates with very narrow nanometre-scale pores.

A promising alternative to these routes is the template-free electrodeposition methodology, which is able to produce similar arrays of small diameter nanowires, but without the need for complex templates, high temperatures or vacuum apparatus. Reaction conditions are chosen in order to provide conditions where the Te growth is guided along a favoured crystal direction by dissolved species such as $SiCl_4$ [7] or halides [8,9], producing wires. To date, this concept has only been demonstrated in ionic liquids, which are often prohibitively expensive, and are complex to synthesise on larger scales for applications working toward upscaling and wider implementation .

For this reason, we moved away from ionic liquids to investigate deep eutectic solvents (DES) as a cost effective alternative for the electrochemical deposition of Te nanowires. DES are made up of complementary pairs of hydrogen bond donors such as urea, glycerol or ethylene glycol, and acceptors, which are most commonly quaternary ammonium halide salts [10]. DES offer similar advantages to ionic liquids, such as high solubility of precursors, high conductivity and a wide solvent window, while also coming at a significantly lower reduced cost [11]. To date, very few investigations have taken advantages of DES for Te electrodeposition in DES [12,13]. These studies were able to produce interesting nanostructures, although these did not facilitate the production nanowires.

To this end, we have explored the electrodeposition of Te in a popular eutectic solvent based on choline chloride and ethylene glycol. Through careful selection of experimental parameters, we were able to produce Te nanowires without the use of templates. Nanowire quality was strongly dependent on the precise reaction conditions, with a

* Corresponding author.
E-mail addresses: s.c.perry@soton.ac.uk (S.C. Perry), iris@soton.ac.uk (I. Nandhakumar).

https://doi.org/10.1016/j.electacta.2022.141674
Received 7 October 2022; Received in revised form 25 November 2022; Accepted 3 December 2022
Available online 5 December 2022
0013-4686/© 2022 The Authors. Published by Elsevier Ltd. This is an open access article under the CC BY license (http://creativecommons.org/licenses/by/4.0/).

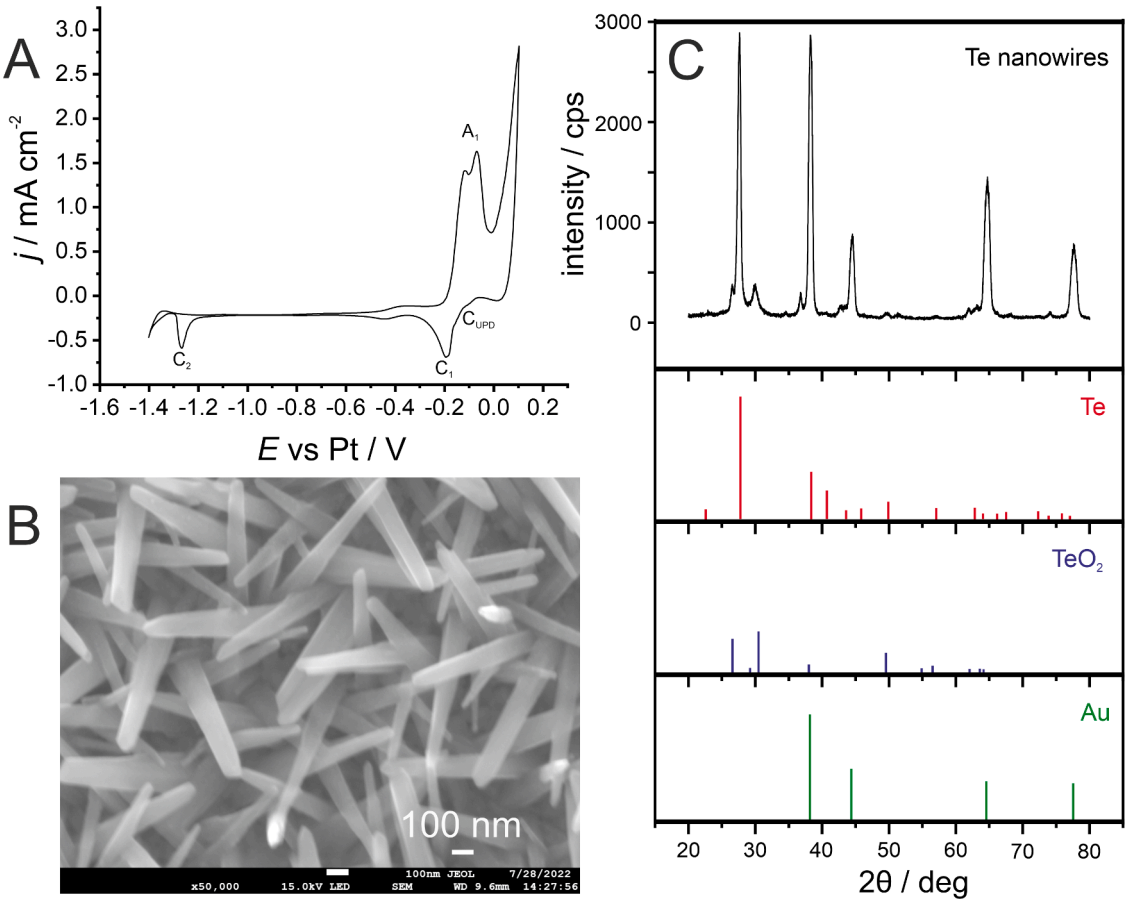

Fig. 1. A) CV for 5 mM $TeCl_4$ in 12CE-Cl at 80 °C, recorded at 10 mV/s at a 2 mm diameter Au electrode. The CV displayed three cathodic peaks corresponding to Te^{IV} reduction to Te^0 (C_1) and Te^0 to Te^{-II} (C_2) and the corresponding anodic oxidation of the Te° film (A_1) Peak C_1 shows a slight shoulder due to the underpotential deposition of Te^0 (C_{UPD}). Sharp increases in the current density at the potential limits demonstrate the solvent window. **B)** Nanowire film obtained through potentiostatic electrodeposition at $E = C_1$ until a total charge $Q = 0.1$ C cm^{-2} had passed. Deposition used the same solution and conditions as for the CV above. **C)** X-Ray Diffraction (XRD) pattern for the tellurium nanowire film shown in B (black), along with patterns corresponding to pure Te (red, ICDD 00–085–0559), TeO_2 (blue, ICDD 00–076–0679) and Au (green, ICDD 00–004–0784).

relatively narrow experimental window producing high quality wires. Interestingly, the film was most strongly dependent on the halide present in solution, with a switch from chloride to iodide-based DES giving access to entirely different nanostructures. We propose that electrodeposition in DES is a simple and efficient route towards multiple nanostructures.

2. Experimental

2.1. Solutions

Solutions for electrodeposition were prepared in a nitrogen flow box (Cleaver Scientific). The chloride-based DES was made by stirring 1 mol % choline chloride (99%, Acros Organic) with 2 mol% ethylene glycol (99.9%, Fisher) at 60 °C until fully dissolved. The choline chloride-based eutectic was designated 12CE-Cl [14]. The same process was used for the production of the bromide and iodide equivalent DES be replacing choline chloride with choline bromide (99%, TCI) or choline iodide (99% Alfa Aesar). These were designated 12CE-Br and 12CE-I respectively. Te solutions for electrodeposition were made by dissolving either $TeCl_4$ (99.9%, Aldrich), $TeBr_4$ (99.9%, Alfa Aesar) or TeI_4 (99.9%, Alfa Aesar) in the matching DES at 80 °C with magnetic stirring.

2.2. Electrode fabrication

All electrodepositions were carried out at a gold working electrode, which were fabricated in house. The glass slide substrates were cleaned by sonicating for 30 mins in Decon® detergent, deionised water and isopropyl alcohol sequentially, and then dried under nitrogen. A 20 nm chromium layer was sputtered onto the glass as an intermediate to aid with the gold adhesion. A 100 nm gold layer was then sputtered onto the chromium to give the finished electrode surface. A glass scribe was used to cut the gold-sputtered slides into 10×25 mm strips. A 10×10 mm area at one end of the strip was used as the electroactive area, with the other end left bare for a crocodile clip to attach.

2.3. Electrochemical measurements

Electrochemical measurements and depositions were performed using a Metrohm μAutolab Type II potentiostat, controlled using Nova 2.1. The electrochemical cell was assembled in a nitrogen flow box with a Pt wire pseudo reference electrode and Pt wire counter electrode. For voltametric analysis, a commercial 2 mm Au working electrode (IJ Cambria) was used to give a well-defined circular geometry. For potentiostatic deposition, the gold-sputtered glass slide electrodes were used for ease of imaging in later stages.

The commercial Au working electrode was cleaned by polishing with 0.3 μm alumina powder prior to each measurement. It was then rinsed well with deionised water before sonicating for 5 mins in deionised water and isopropyl alcohol and dried under nitrogen. Gold slide electrodes were not polished due to the thin gold layer, and so were cleaned by sonicating for 5 mins in Decon® detergent, deionised water and

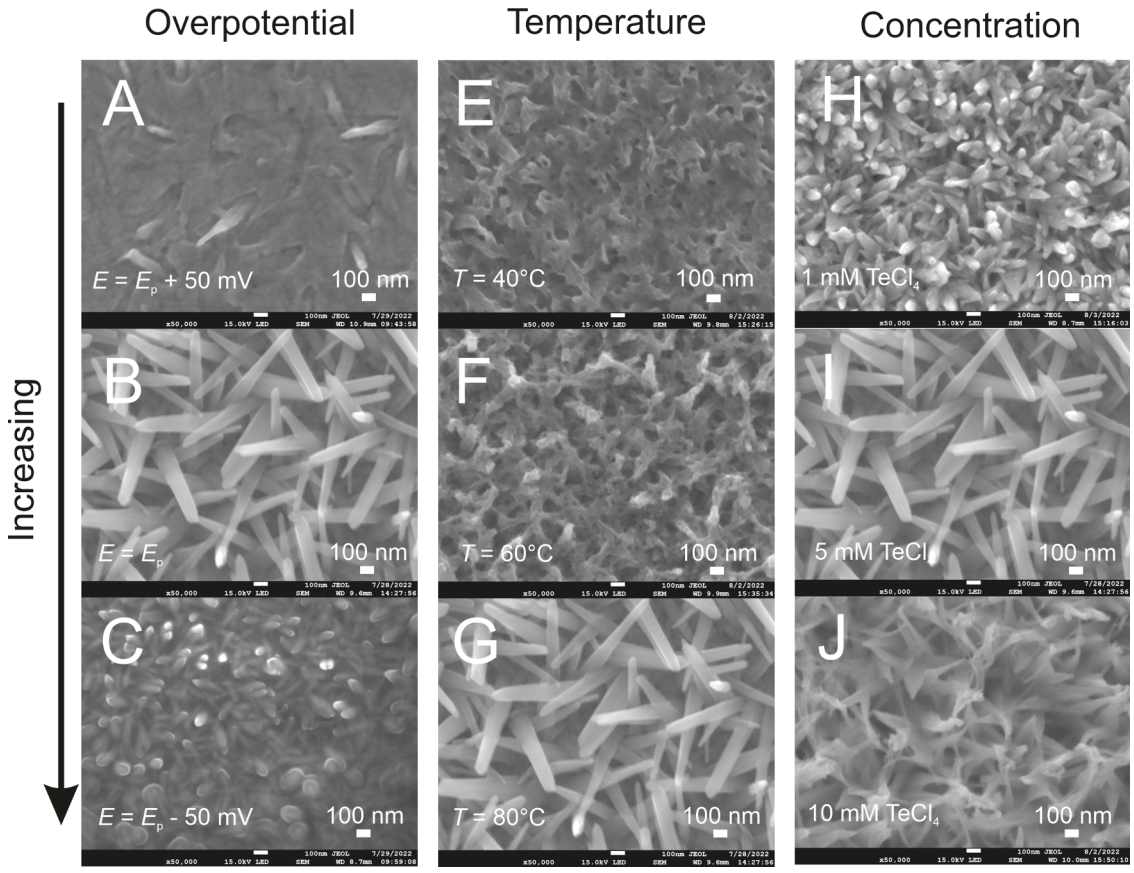

Fig. 2. Impact of varied solution conditions on the quality of Te nanostructure obtained by electrochemical deposition of $TeCl_4$ in 12CE-Cl. All depositions show the same charge passed, $Q = 0.1$ C cm^{-2}. **Left column)** Impact of making the deposition potential more negative, thereby increasing overpotential from $E_p + 50$ mV (A) to E_p (B) and $E_p - 50$ mV (C). **Centre column)** Impact of increasing the temperature from 40 °C (E) to 60 °C (F) and 80 °C (G). **Right column)** Impact of increasing the concentration of $TeCl_4$ from 1 mM (H) to 5 mM (I) and 10 mM (J).

isopropyl alcohol sequentially, and then dried under nitrogen. A Pt wire was used as a pseudo reference rather than the commonly employed Ag wire to avoid any potential dissolution of Ag during potentiostatic deposition that could result in co-deposition [9].

Electrochemical measurements and depositions themselves were carried out at the lab bench, so dissolved oxygen and water concentrations are expected to be low, but present. The cell was heated to the desired temperature in a thermostatically controlled oil bath. All electrochemical depositions were performed potentiostatically until a total charge of 0.1 C cm^{-2} had passed.

2.4. Imaging and characterisation

Images of the nanowire films and elemental analysis were recorded on a Jeol JSM-7200F scanning electron microscope (SEM), which has energy dispersive X-ray (EDX) capability. The crystalline structure was also investigated by Xray diffraction (XRD) using a Rigaku Smartlab Xray diffractometer with CuK_α radiation. Samples were scanned from a 2θ of 10° - 80° with a step size of 10° min^{-1}. The XRD spectra were then analysed in PDXL2 and compared against reference spectra from the International Centre of Diffraction Data (ICDD) database.

3. Results

3.1. Te nanowire growth in 12CE-Cl

In order to determine the electrochemical behaviour of Te in 12CE-Cl, a gold electrode was cycled at 10 mV/s until a stable voltammogram was observed (Fig. 1). The resultant cyclic voltammogram (CV) showed reduction peaks associated with the initial reduction of tellurium cation to metallic tellurium at low overpotential (C_1). Peak C_1 also shows a slight shoulder, which has been demonstrated to be due to the underpotential deposition of Te^0 [15].

$$Te^{IV} + 4e^- \rightleftharpoons Te^o \quad (1)$$

Cycling at faster scan rates causes a slight drift of C_1 to more negative potentials (ESI, Fig S1), indicating the quasi-reversibility of this process [16]. At much more negative potentials, a further reduction peak signifies the reduction of Te^0 to give the telluride anion [8].

$$Te^o + 2e^- \rightleftharpoons Te^{-II} \quad (2)$$

Sweeping to more positive potentials revealed anodic peaked corresponding to the oxidative stripping of the previously deposited Te film (A_1). The first depositions were recorded at −0.2 V vs. Pt, corresponding to reduction peak C_1.

Surprisingly, a simple electrodeposition in 12CE-Cl produced Te nanowires without the need for any additional liquid or solid phase template in the experimental design. The obtained nanowires were approximately 70 nm in diameter and 1 μm in length, with good coverage over the entirety of the gold electrode surface. X-ray diffraction (XRD) analysis (Fig. 2) confirmed the production of a pure tellurium phase, with sharp peaks indicating a high degree of crystallinity. A small amount of oxidation was also observed, which likely occurred in the transfer between deposition bath and analysis, which was under ambient conditions. This was confirmed via elemental analysis (ESI Fig S2), which showed a pure tellurium phase with a low level oxygen content. Further parameterisation was then performed in order to investigate the impact of deposition conditions on the obtained

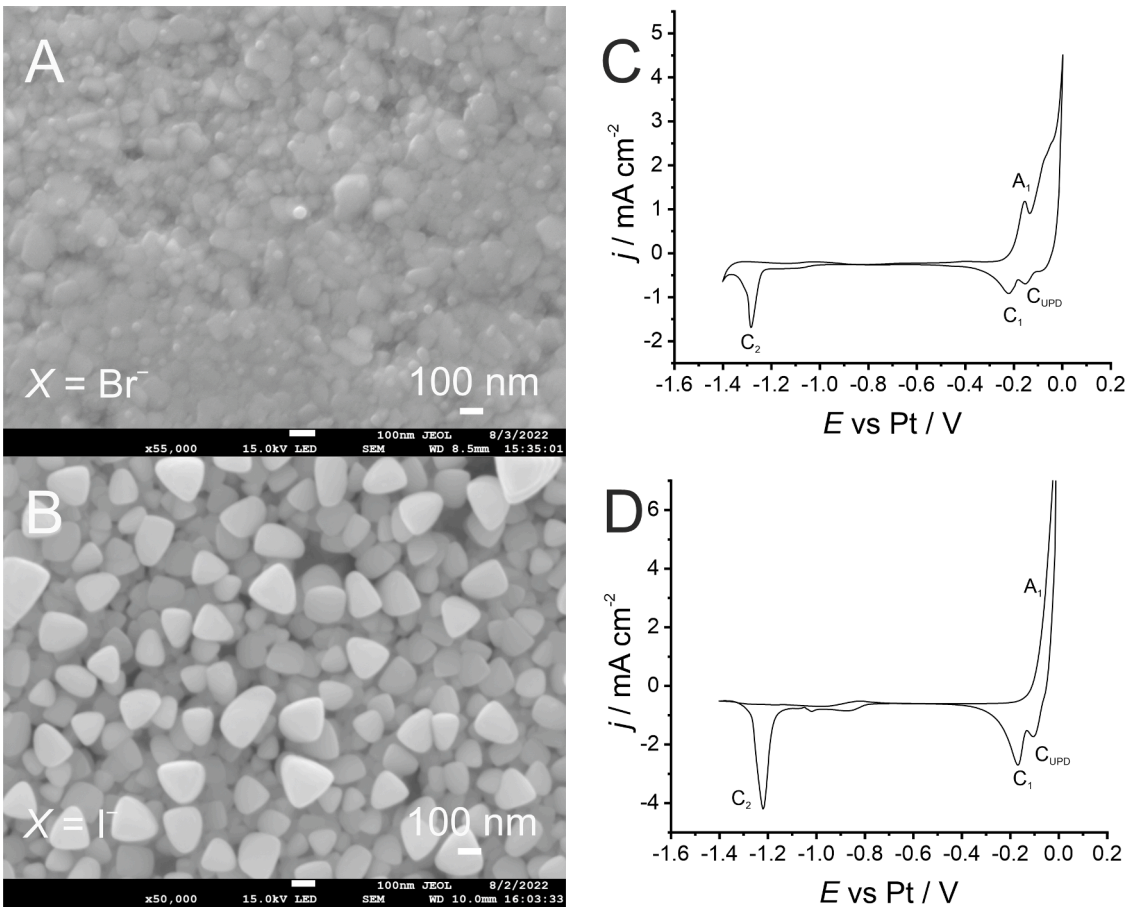

Fig. 3. Left) Tellurium electrodeposition from a solution of **A)** 5 mM $TeBr_4$ in 12CE-Br at 80 °C and **B)** 5 mM TeI_4 in 12CE-I at 80 °C. Both depositions were done at −0.2 V vs. Pt until a total charge $Q = 0.1$ C cm^{-2}. **Right)** CVs recorded at 20 mV/s on a 2 mm diameter Au electrode in **C)** 5 mM $TeBr_4$ in 12CE-Br at 80 °C and **D)** 5 mM TeI_4 in 12CE-I at 80 °C, matching the same experimental conditions as were used to produce the images in A and B respectively. The peak potential for Te^{IV} reduction (C_1) can be seen to be in the same place (−0.2 V vs. Pt) in both cases.

nanowires.

3.2. Variations in the deposition conditions

The same experimental setup was used to electrochemically deposit Te films under a range of concentrations, temperatures and applied potentials in order to ascertain how experimental conditions impacted the quality of the Te nanostructure (Fig. 2). The precise deposition conditions clearly has a stark impact on the quality of the Te nanostructure that may be obtained using this method. The applied potential capable of producing wires is narrow, with deviations of 50 mV leaving some wire-like features observable in places, though these are much more poorly defined compared to those recorded at $E = C_1$.

When the temperature of the bath is decreased, features of the nanostructure becomes thinner and more fused, with lower temperatures giving a structure that more resembles a porous sponge than an array of nanowires. Similarly, decreasing the concentration of $TeCl_4$ from 5 to 1 mM gave a much more tightly packed array of thinner, shorter wires. Since the deposition charge is the same in all cases, the change in wire size and length cannot be ascribed to the total charge passed. Instead, these differences appear to be related to the mobility of Te in solution. Te nanostructure growth is largely defined either by the formation of nucleation sites or the nature of growth once nucleation has occurred. A decrease in Te availability, whether by low temperature slowing mass transfer or low concentration decreasing the molarity, would slow the growth rate from initial nucleation sites, which seems to result in thinner nanostructures that are more likely to fuse. There seems to be an optimum mobility range for the formation of nanowires over other structures, since further increase in $TeCl_4$ concentration to 10 mM results in a much less defined nanostructure.

3.3. Impact of halides on wire growth

The growth of wires in the 12CE-Cl DES was hypothesised to be due to a templating impact coming from the high concentration of halide ions in the DES providing a templating impact during the deposition. To investigate this further, we produced DES using choline bromide (12CE-Br) and choline iodide (12CE-I) in place of the choline chloride. All other parameters for the production of solutions and for the deposition procedures were kept the same. Cyclic voltammetry was used to check the impact of changing the halide on the electrochemistry of the Te^{4+} cation. In both cases, the CVs were very similar, with the exception that the anodic peaks corresponding to Te^0 oxidation were less well defined due to interference from Br^- and I^- oxidation, which is more facile compared to Cl^- oxidation [17]. Most importantly, the deposition peak (C_1) can be seen at the same potential (Fig. 3C-D). Depositions were therefore done at the same potential for 5 mM $TeBr_4$ in 12CE-Br and for 5 mM TeI_4 in 12CE-I until 0.1 C cm^{-2} had passed (Fig. 3).

Fig. 3 shows a remarkable impact of the choice of halide on the resultant nanostructure, despite deposition conditions being otherwise identical. The use of bromide as the anion results in a film with no clearly defined nanostructure that was also more susceptible to delamination than films produced in the other DES. The use of iodide changes the film entirely to give structures more reminiscent of nanoplatelets, with diameters ranging between 100 and 300 nm. This shows a clear impact of the halide on the nature of nanostructure obtainable during

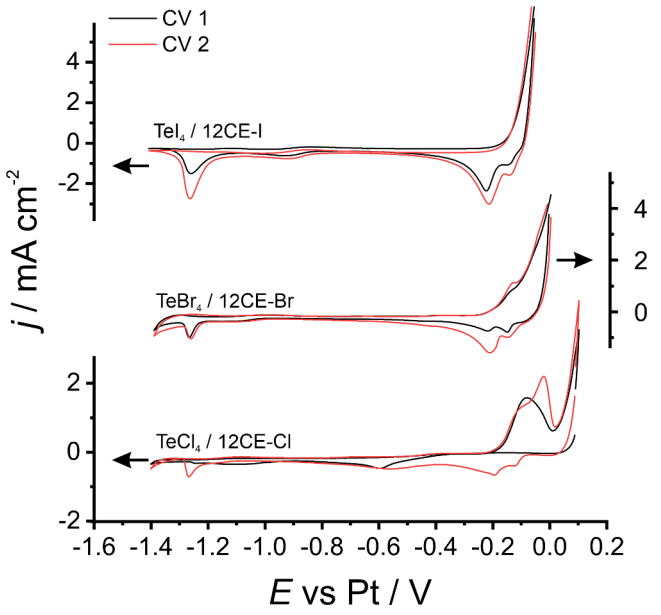

Fig. 4. CV for 5 mM TeX_4 in 12CE-X, where X is I (top), Br (middle) and Cl (bottom). The first scan (black) was recorded immediately after assembling the cell following polishing and cleaning the gold working electrode. The second scan (black) immediately followed the first. All CVs were recorded at a 2 mM diameter Au working electrode at 50 mV/s in a thermostatically controlled bath at 80 °C.

electrodeposition.

Altering the halide in the DES has the potential to impact the Te nucleation step, the nature of Te film growth, and the properties of the DES itself. Recent works in brominated ionic liquids have indicated that halides do not play a role as capping agents in the formation of nanowires during tellurium electrodeposition [9]. Other works instead suggested halides can favour adsorption of Te adatoms at specific sites that favour certain nanostructures, [8] and strongly adsorbing anions have been shown to give smaller crystallite sizes in Cd deposition [18]. It therefore seems likely that the choice of halide alters the resultant nanostructure by altering the substrate-solution interface in the nucleation phase of the electrodeposition.

A key feature of choline-based DES is the adsorption of the choline cations at the substrate surface. This has been observed at both open circuit and negative potentials [19], and has been shown to be especially strong for gold substrates [20]. The adsorption of cations in ionic liquids can hinder nucleation events in electrodeposition [21]. The impact of this can be clearly seen when comparing the first CV to subsequent CVs during repeated cycling (Fig. 4).

In the case of 12CE-Cl, the first CV shows that the reduction peak corresponding to Te^{IV} reduction to Te^0 is significantly more negative than is seen in subsequent scans. The key difference is that the second and subsequent CVs will have some remaining Te^0 over the gold substrate due to the incomplete oxidation during the forward sweep. This indicates a significant kinetic limitation in the initial nucleation, since the deposition overpotential is greatly decreased when some Te^0 is already present at the electrode surface.

This suggests a mode of electrodeposition in 12CE-Cl where the initial nucleation occurs by underpotential deposition. Further electrodeposition will then preferentially occur at these sites rather than bare Au sites, leading to the growth of nanowires in place of smooth film formation. The crystal structure of Te is highly anisotropic, and has a natural tendency to grow into low dimensional nanowire or nanoplatelet structures depending on the reaction environment [4,22]. It therefore seems likely that the passivation of the gold surface by adsorbed choline cations is sufficient to produce nanowires, since electrochemical growth will be favoured at nucleated Te sites over the passivated substrates, and the low overpotential deposition will allow Te to grow along the favoured c axis to give nanowires. This is in agreement with the narrow potential window for wire formation seen in Fig. 2, since the overpotential must be low enough to allow the Te to grow along its preferred axis.

Importantly, this distinction between CV 1 and CV 2 during repeated cycling is not seen in the presence of Br^- or I^- based DES, so that peak C_1 is at the same potential for all scans. Tellurium electrodeposition at the bare Au electrode therefore appears to be as kinetically facile as for an Au surface with existing Te nucleation sites. This suggests that halides have the ability to disrupt the adsorbed choline layer so that it does not have the same passivating impact, such that Te reduction may proceed unimpeded.

The structure of the substrate-solution interface in DES has the adsorbed cation layer followed by alternating anion and cation layers [23]. However, this ordered structure has been shown to be disrupted by metal halides [24]. Electrodeposition of a metal halide would result in an accumulation of the halide at the electrode surface around the nucleation sites and areas of metal growth [25]. Spectroscopic data has suggested Te^{IV} exists predominantly as $TeCl_6^{2-}$ [15,26], so deposition of Te would result in a sizeable accumulation of Cl^- at the electrode surface, following Eq. (3).

$$TeCl_6^{2-} + 4e^- \rightleftharpoons Te^0 + 6Cl^- \quad (3)$$

Disruption of the choline layer by Cl^- could cause free Au sites to be revealed, facilitating deposition a lower overpotentials and subsequent nanowire growth. Given the significant shift in C_1 between the first and second CVs in Fig. 4, Cl^- could be expected to give only a minimal disruption, revealing few opportunities for Te deposition and therefore facilitating wire growth from spare nucleation sites. It follows that variations in the disruption of choline layer by Cl^-, Br^- and I^- anions due to their different size and electronegativity would alter the nature of the nucleation and growth of the electrodeposited Te, leading to the observed changes in nanostructure.

4. Conclusions

We have demonstrated the electrodeposition of tellurium nanostructures using DES. Using the chloride-based 12CE-Cl DES, we demonstrated that taking steps to decrease the availability of Te^{4+} to the electrode surface, such as through decreased concentration or temperature, leads to smaller geometries in the resultant nanostructures, although this also allows neighbouring nanostructures to become fused leading to a more complex film structure. The operating window where nanowires were seen evenly distributed over the surface was surprisingly narrow, requiring a deposition potential corresponding to the peak reduction potential obtainable via cyclic voltammetry.

We have also showed that halide analogues of the DES employing bromide and iodide choline salts result in vastly different nanostructures, with Br^- producing films with no clear nanostructure, whereas I^- led to the formation of platelet structures in place of the previously observed wires. The key difference in the DES studied is seen in the difference between the first and subsequent CVs during repeated cycling. Chloride-based CVs show a reduction peak for Te^{IV} at very large overpotential, which is then replaced by one at much lower overpotential on subsequent scans. We propose this is due to the adsorption of choline cations at the gold surface hindering the initial reduction of Te. This passivating adsorption layer means that Te preferentially deposits at existing nucleation sites, facilitating nanowire growth. Replacing Cl^- with either Br^- or I^- disrupts this layer, leading to the formation of alternative Te morphologies. This offers DES as promising a solvent for template-free production of metallic nanowires and nanoplatelets.

CRediT authorship contribution statement

Samuel C. Perry: Conceptualization, Methodology, Investigation, Writing – original draft. **Joshua White:** Investigation, Writing – review & editing. **Iris Nandhakumar:** Writing – review & editing.

Declaration of Competing Interest

The authors declare that they have no known competing financial interests or personal relationships that could have appeared to influence the work reported in this paper.

Acknowledgements

This work was financially supported by the Engineering and Physical Sciences Research Council (EPSRC) Grant No. EP/T026219/1. The authors would also like to thank Nikolay Zhelev for assistance in the preparation of the gold coated glass electrodes in this work, and the University of Southampton Glassblowers for producing custom fritted glass electrode bodies for reference electrode fabrication.

Supplementary materials

Supplementary material associated with this article can be found, in the online version, at doi:10.1016/j.electacta.2022.141674.

References

[1] S. Lin, W. Li, Z. Chen, J. Shen, B. Ge, Y. Pei, Tellurium as a high-performance elemental thermoelectric, Nat. Commun. 7 (2016) 10287.
[2] Z. Shi, R. Cao, K. Khan, A.K. Tareen, X. Liu, W. Liang, Y. Zhang, C. Ma, Z. Guo, X. Luo, H. Zhang, Two-Dimensional Tellurium: progress, Challenges, and Prospects, Nano-Micro Lett 12 (2020) 99.
[3] G. Qiu, A. Charnas, C. Niu, Y. Wang, W. Wu, P.D. Ye, The resurrection of tellurium as an elemental two-dimensional semiconductor, npj 2D Mater. Appl. 6 (2022) 17.
[4] Z. He, Y. Yang, J.-.W. Liu, S.-.H. Yu, Emerging tellurium nanostructures: controllable synthesis and their applications, Chem. Soc. Rev. 46 (2017) 2732–2753.
[5] A. Amin, R. Huang, D. Newbrook, V. Sethi, S. Yong, S. Beeby, I. Nandhakumar, Screen-printed bismuth telluride nanostructured composites for flexible thermoelectric applications, J. Phys. Energy 4 (2022), 024003.
[6] P.N. Bartlett, D.A. Cook, M.M. Hasan, A.L. Hector, S. Marks, J. Naik, G. Reid, J. Sloan, D.C. Smith, J. Spencer, Z. Webber, Supercritical fluid electrodeposition, structural and electrical characterisation of tellurium nanowires, RSC Adv 7 (2017) 40720–40726.
[7] R. Al-Salman, H. Sommer, T. Brezesinski, J. Janek, Template-free electrochemical synthesis of high aspect ratio Sn nanowires in ionic liquids: a general route to large-area metal and semimetal nanowire arrays? Chem. Mater. 27 (2015) 3830–3837.
[8] J. Szymczak, S. Legeai, S. Diliberto, S. Migot, N. Stein, C. Boulanger, G. Chatel, M. Draye, Template-free electrodeposition of tellurium nanostructures in a room-temperature ionic liquid, Electrochem. Commmun. 24 (2012) 57–60.
[9] L. Thiebaud, S. Legeai, J. Ghanbaja, N. Stein, Electrodeposition of high aspect ratio single crystalline tellurium nanowires from piperidinium-based ionic liquid, Electrochim. Acta 222 (2016) 528–534.
[10] T. El Achkar, H. Greige-Gerges, S. Fourmentin, Basics and properties of deep eutectic solvents: a review, Environ. Chem. Lett. 19 (2021) 3397–3408.
[11] B.B. Hansen, S. Spittle, B. Chen, D. Poe, Y. Zhang, J.M. Klein, A. Horton, L. Adhikari, T. Zelovich, B.W. Doherty, B. Gurkan, E.J. Maginn, A. Ragauskas, M. Dadmun, T.A. Zawodzinski, G.A. Baker, M.E. Tuckerman, R.F. Savinell, J. R. Sangoro, Deep eutectic solvents: a review of fundamentals and applications, Chem. Rev. 121 (2021) 1232–1285.
[12] C. Agapescu, A. Cojocaru, A. Cotarta, T. Visan, Electrodeposition of bismuth, tellurium, and bismuth telluride thin films from choline chloride–oxalic acid ionic liquid, J. Appl. Electrochem. 43 (2013) 309–321.
[13] L.P.M. dos Santos, R.M. Freire, S. Michea, J.C. Denardin, D.B. Araújo, E.B. Barros, A.N. Correia, P. de Lima-Neto, Electrodeposition of 1-D tellurium nanostructure on gold surface from choline chloride-urea and choline chloride-ethylene glycol mixtures, J. Mol. Liq. 288 (2019), 111038.
[14] L. Vieira, J. Burt, P.W. Richardson, D. Schloffer, D. Fuchs, A. Moser, P.N. Bartlett, G. Reid, B Gollas, Tin, bismuth, and tin–bismuth alloy electrodeposition from chlorometalate salts in deep eutectic solvents, ChemistryOpen 6 (2017) 393–401.
[15] A. Sorgho, M. Bougouma, G. De Leener, J. Vander Steen, T. Doneux, Impact of speciation on the tellurium electrochemistry in choline chloride-based deep eutectic solvents, Electrochem. Commmun. 140 (2022), 107327.
[16] A.-.S. Catrangiu, I. Sin, P. Prioteasa, A. Cotarta, A. Cojocaru, L. Anicai, T. Visan, Studies of antimony telluride and copper telluride films electrodeposition from choline chloride containing ionic liquids, Thin Solid Films 611 (2016) 88–100.
[17] Q. Li, J. Jiang, G. Li, W. Zhao, X. Zhao, T. Mu, The electrochemical stability of ionic liquids and deep eutectic solvents, Sci. China Chem. 59 (2016) 571–577.
[18] Y. Mastai, D. Gal, G. Hodes, Nanocrystal-size control of electrodeposited nanocrystalline semiconductor films by surface capping, J. Electrochem. Soc. 147 (2000) 1435.
[19] L. Vieira, R. Schennach, B. Gollas, In situ PM-IRRAS of a glassy carbon electrode/deep eutectic solvent interface, Phys. Chem. Chem. Phys. 17 (2015) 12870–12880.
[20] M. Figueiredo, C. Gomes, R. Costa, A. Martins, C.M. Pereira, F. Silva, Differential capacity of a deep eutectic solvent based on choline chloride and glycerol on solid electrodes, Electrochim. Acta 54 (2009) 2630–2634.
[21] L. Vieira, R. Schennach, B. Gollas, The effect of the electrode material on the electrodeposition of zinc from deep eutectic solvents, Electrochim. Acta 197 (2016) 344–352.
[22] A.B. Pun, S. Mazzotti, A.S. Mule, D.J. Norris, Understanding discrete growth in semiconductor nanocrystals: nanoplatelets and magic-sized clusters, Acc. Chem. Res. 54 (2021) 1545–1554.
[23] R. Hayes, N. Borisenko, M.K. Tam, P.C. Howlett, F. Endres, R. Atkin, Double layer structure of ionic liquids at the Au(111) electrode interface: an atomic force microscopy investigation, J. Phys. Chem. C 115 (2011) 6855–6863.
[24] R. Hayes, N. Borisenko, B. Corr, G.B. Webber, F. Endres, R. Atkin, Effect of dissolved LiCl on the ionic liquid–Au(111) electrical double layer structure, Chem. Commun. 48 (2012) 10246–10248.
[25] Y.-.T. Hsieh, M.-.C. Lai, H.-.L. Huang, I.W. Sun, Speciation of cobalt-chloride-based ionic liquids and electrodeposition of Co wires, Electrochim. Acta 117 (2014) 217–223.
[26] E.G.S. Jeng, I.W. Sun, Electrochemistry of Tellurium(IV) in the basic aluminum chloride-1-methyl-3-ethylimidazolium chloride room temperature molten salt, J. Electrochem. Soc. 144 (1997) 2369.